Polyhedron 69 (2014) 61–67

Contents lists available at ScienceDirect

Polyhedron

journal homepage: www.elsevier.com/locate/poly

Chemistry of gold(III) with pyridine-carboxamide ligands

Nasser Nasser, Richard J. Puddephatt *

Department of Chemistry, University of Western Ontario, London N6A 5B7, Canada

ARTICLE INFO

Article history:
Received 2 October 2013
Accepted 22 November 2013
Available online 1 December 2013

Keywords:
Gold
Pyridine-carboxamide
Amide
Catalysis

ABSTRACT

The pyridine-carboxamide ligand PhNHC(=O)—2-C_5H_4N reacts with $Na^+[AuCl_4]^-$ either by cation exchange, to give [PhNHC(=O)—2-C_5H_4NH][$AuCl_4$], or by ligand substitution to give [$AuCl_2$(κ^2-*N*,*N*′-PhNC(=O)—2-C_5H_4N)]. Similar reactions with bis(pyridine-carboxamide) ligands gave complexes [$AuCl_2$(κ^2-*N*,*N*′-RNC(=O)—2-C_5H_4N)], with R = $(CH_2)_3$NHC(=O)—2-C_5H_4N or 2-C_6H_4NHC(=O)—2-C_5H_4N, in which the ligands are bidentate, but no complexes with tetradentate ligands could be isolated. The complex [$AuCl_2$(κ^2-*N*,*N*′-PhNC(=O)—2-C_5H_4N)] in methanol solution is an efficient catalyst for oxidative cyanation of $PhNMe_2$ to give $PhMeNCH_2CN$, and it is proposed that the catalysis involves gold(I), gold(II) and gold(III) intermediates.

1. Introduction

Transition metal complexes with pyridine-carboxamide ligands have been shown to have useful properties in catalysis or molecular materials, and could be useful as pharmaceuticals or photonic materials [1–3]. In catalysis, the ligands are particularly useful in oxidation reactions since they are not themselves easily oxidized, and also in biological systems since the carboxamide groups are compatible with proteins [4–6]. Gold complexes are also useful in catalysis, biology and molecular materials [7–10], yet there are relatively few reports of complexes of gold with pyridine-carboxamide or related ligands [3,11–16]. Some of these are shown in Chart 1. Coordination occurs with deprotonation of the amide group and it has been suggested that this leads to enhanced stability of the chelate complex [17,18]. The effect has been used to selectively adsorb gold(III) on protein materials [19]. Simple 2-pyridyl-carboxamide ligands give neutral complexes such as **A** or **B** (Chart 1), while bridged bis(2-pyridyl-carboxamide) ligands can act as tetradentate ligands, as in **C**, or as bidentate ligands, as in **D** [11–15].

In earlier papers, we have been interested in developing the chemistry of gold with bis(phosphine-carboxamide) ligands [20–22]. These ligands favor the oxidation state gold(I) and the amide group usually does not coordinate but may take part in hydrogen bonding. In attempts to use the gold(I) complexes in oxidation catalysis, the phosphine donors were often oxidized to phosphine oxides, which are not good ligands for gold. Pyridine-carboxamide ligands have been used in supramolecular chemistry with late transition metals [2,23–26] and, since they are not easily oxidized [4], it was of interest to study their chemistry with gold(I) and gold(III) and to test the catalytic activity of the complexes formed. The results are reported below.

2. Experimental

2.1. Materials and methods

All reactions were carried out in inert atmosphere of dry nitrogen using standard Schlenk techniques, unless otherwise specified. All solvents used for air and moisture sensitive materials were purified using an innovative Technology Inc. *PURE SOLV* solvent purification system (SPS). NMR spectra were recorded at ambient temperature, unless otherwise noted (ca. 25 °C), on Varian Mercury 400 or Varian Inova 400 or 600 spectrometers. ^{1}H chemical shifts are reported relative to TMS (^{1}H), 85% H_3PO_4. Mass spectrometric analysis was carried out using an electrospray PE-Sciex Mass Spectrometer (ESI-MS) coupled with TOF detector. For X-ray structure determination, a suitable crystal of each compound was coated in Paratone oil and mounted on a glass fiber loop. X-ray data were collected at 150 K with ω and φ scans by using a Bruker Smart Apex II diffractometer with graphite-monochromated Mo Kα radiation (λ = 0.71073 Å) and Bruker SMART software [27]. Unit cell parameters were calculated and refined from the full data set. Cell refinement and data reduction were performed using the Bruker APEX2 and SAINT programs respectively [28]. Reflections were scaled and corrected for absorption effects using SADABS [29]. All structures were solved by either Patterson or direct methods with SHELXS and refined by full-matrix least-square techniques against F^2 using SHELXL [30]. All non-hydrogen atoms were refined anistropically. The hydrogen atoms were placed in calculated positions and refined using the riding model. Crystal data are summarized in

* Corresponding author.
E-mail address: pudd@uwo.ca (R.J. Puddephatt).

0277-5387/$ - see front matter © 2013 Elsevier Ltd. All rights reserved.
http://dx.doi.org/10.1016/j.poly.2013.11.022

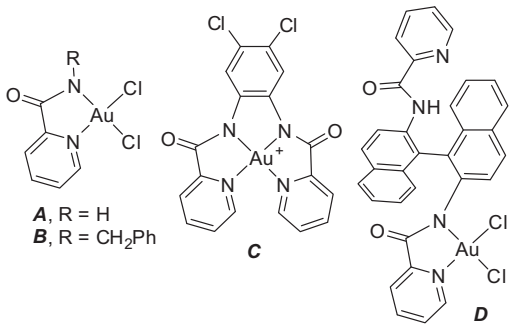

Chart 1. 2-Pyridine-carboxamide complexes of gold(III).

Table 1 and in the CIF files (CCDC 964344–964346). DFT calculations were carried out by using the Amsterdam Density Functional program based on the BLYP functional, with double-zeta basis set and first-order scalar relativistic corrections [31]. The ligands 1,2-C_6H_4(NHCO–2-$C_5H_4N)_2$ and CH_2(CH_2NHCO–2-$C_5H_4N)_2$ were prepared by the literature method [32,33].

2.2. Synthesis of new complexes

2.2.1. [$AuCl_2$(2-C_5H_4N—C(=O)NPh]

To a solution of PhNHC(=O)—2-C_5H_4N (0.05 g, 0.25 mmol) in THF (5 mL) was added a solution of $NaAuCl_4{\cdot}2H_2O$ (0.10 g, 0.25 mmol) in THF (5 mL). Excess Na_2CO_3 (0.3 g) was added to the reaction mixture, which was allowed to stir for 12 h, then filtered to remove insoluble material. The solvent was evaporated under vacuum, and the red solid product was washed with *n*-pentane and diethyl ether and dried under vacuum. Yield: 0.09 g (78%). NMR in DMSO-d_6 at 400 MHz: $\delta(^1H)$ = 9.37 [d, 1H, $^3J_{HH}$ = 7 Hz, H^6], 8.56 [t, 1H, $^3J_{HH}$ = 7 Hz, H^5], 8.05–8.13 [m, 2H, H^3, H^4], 7.29–7.39 [m, 5H, Ph]. *Anal.* Calc. for $C_{12}H_9AuCl_2N_2O$: C, 30.99; H, 1.95; N, 6.02. Found: C, 30.54; H, 1.73; N, 5.68%. Single crystals were grown by the slow diffusion of pentane into a solution of the sample dissolved in a mixture of methanol, dichloromethane, chloroform and acetone.

In a similar synthesis, but with stoichiometric amount of Na_2CO_3, recrystallization gave a mixture of red crystals of the above complex with pale yellow crystals, identified as [PhNHC(=O)—2-$C_5H_4NH]^+[AuCl_4]^-$ by X-ray structure determination.

2.2.2. [$AuCl_2${1,2-C_6H_4(NCO–2-C_5H_4N)(NHCO–2-C_5H_4N)}]

This was prepared in a similar way from 1,2-C_6H_4(NHCO–2-$C_5H_4N)_2$ (0.050 g, 0.16 mmol) and $NaAuCl_4{\cdot}2H_2O$ (0.063 g, 0.16 mmol) and isolated as a red solid. Yield: 0.082 g (89%). NMR in DMSO-d_6 at 400 MHz: $\delta(^1H)$ = 10.48 [s, 1H, NH], 9.46 [d, 1H, $^3J_{HH}$ = 7 Hz, H^6], 8.62 [d, 1H, $^3J_{HH}$ = 7 Hz, H^3], 8.41 [d, 1H, $^3J_{HH}$ = 7 Hz, $H^{6'}$], 8.31 [d, 1H, $^3J_{HH}$ = 7 Hz, $H^{3'}$], 8.1–8.2 [m, 4H], 7.1–7.6 [m, 4H]. *Anal.* Calc. for $C_{18}H_{13}AuCl_2N_4O_2$: C, 36.94; H, 2.24; N, 9.57. Found: C, 36.46; H, 1.80; N, 9.23%. Single crystals were grown by slow diffusion of *n*-pentane into a methanol solution of the compound.

2.2.3. [$AuCl_2${CH_2(CH_2NCO–2-C_5H_4N)(CH_2NHCO–2-C_5H_4N)]

This was prepared in a similar way from CH_2(CH_2NHCO–2-$C_5H_4N)_2$ (0.050 g, 0.18 mmol) and $NaAuCl_4{\cdot}2H_2O$ (0.070 g, 0.18 mmol) and isolated as a yellow solid. Yield: 0.090 g (93%). NMR in DMSO-d_6 at 400 MHz: $\delta(^1H)$ = 9.28 [d, 1H, H^6], 8.82 [t, 1H, NH], 8.62 [d, 1H, $H^{6'}$], 8.50 [t, 1H, H^5], 7.95–8.04 [m, 3H, H^3, H^4, $H^{3'}$], 7.56–7.60 [m, 2H, $H^{4'}$, $H^{5'}$], 3.55 [m, 2H, CH_2N], 3.36 [m, 2H, CH_2N], 1.84 [quin, 2H, CH_2]. *Anal.* Calc. for $C_{15}H_{15}AuCl_2N_4O_2$: C, 32.69; H, 2.74; N, 10.16. Found: C, 32.27; H, 2.71; N, 9.75%. Single crystals were grown by slow diffusion of *n*-pentane into a dichloromethane solution of the compound.

2.3. Catalysis

To a stirred solution of *N*,*N*-dimethylaniline (0.96 g, 7.9 mmol) in methanol (15 mL) was added [$AuCl_2$(2-C_5H_4N—C(=O)NPh] (0.18 g, 0.39 mmol), followed by *t*-BuOOH (9.5 mmol, as a 5 M solution in decane) and Me_3SiCN (1.97 mL, 15.8 mmol). The reaction was allowed to stir until all *N*,*N*-dimethylaniline was consumed (5 h, monitored by TLC), then quenched by addition of excess aqueous $NaHCO_3$. The mixture was extracted with ethyl acetate, the combined organic layer was washed with brine, dried over anhydrous $MgSO_4$, and the solvent was removed under reduced pressure to give the product PhMeNCH_2CN (1.1 g, 95%). NMR in $CDCl_3$: $\delta(^1H)$ = 7.35 [m, 2H, Ph-*o*]; 6.98 [t, 1H, Ph-*p*]; 6.91 [m, 2H, Ph-*m*]; 4.14 [s, 2H, CH_2CN]; 2.99 [s, 3H, CH_3]. ESI-MS: *m*/*z* = 146.

In attempts to identify intermediates, the reactions in $CDCl_3$ were monitored by ^1H NMR spectroscopy. Reagents were added in different sequences and NMR spectra were recorded at each stage. Yields of volatile products in the final solutions were determined by GC–MS and less volatile products were identified by ESI-MS. In a typical experiment, to a solution of $PhNMe_2$ (24 mg, 0.2 mmol) in $CDCl_3$ (0.2 mL) was added a solution of [$AuCl_2$(2-C_5H_4N–C(=O)NPh] (4.5 mg, 9.7 μmol) in $CDCl_3$ (0.1 mL). The solution immediately became violet-blue in color. In the ^1H NMR, the *m* and *p*-phenyl resonances which overlap at δ 6.77–6.81 in free $PhNMe_2$ gave broad resonances shifted to 6.85 [1H, *m*] and 6.94

Table 1
Crystal and refinement data.

Complex	**4**	**5**	**6**
Formula	$C_{12}H_{11}AuCl_4N_2O$	$C_{12}H_9AuCl_2N_2O$	$C_{15}H_{15}AuCl_2N_4O_2$
Fw	537.99	465.08	551.18
Crystal system	monoclinic	monoclinic	monoclinic
Space group	$P2_1/n$	$P2_1/c$	$C2/c$
a	8.8311(3)	16.1441(17)	29.0237(13)
b	7.5187(3)	16.8323(17)	7.9773(4)
c	23.3384(8)	9.6879(9)	18.0225(9)
β	100.880(2)	92.914(3)	126.3750(10)
Z	4	8	8
V	1521.78(10)	2629.2(5)	3359.7(3)
D_{calc}	2.348	2.350	2.179
μ (mm^{-1})	10.364	11.584	9.092
Reflection/restraint/parameter	3358/0/181	6037/0/325	4167/0/217
R_1, $I > 2\sigma(I)$	0.0186	0.0423	0.0165
wR_2 (all data)	0.0382	0.0859	0.0397

[2H, *p*]. Some free ligand PhNHC(=O)–2-C_5H_4N was also detected. After 1 h, a solution of Me_3SiCN (50 μL, 0.4 mmol) in $CDCl_3$ (0.1 mL) was added. Reaction occurred to give Me_3SiCl [$\delta(^1H) = 0.4$ ppm] and $(Me_3Si)_2O$ [$\delta(^1H) = 0.023$] and more free ligand was formed. The $PhNMe_2$ resonances returned to their normal positions. After 1 h, *t*-BuOOH (0.24 mmol) in $CDCl_3$ (0.1 mL) was added. The chief changes were decay of resonances for Me_3SiCN and Me_3SiCl, along with an increase in resonances for Me_3SiOH [$\delta(^1H) = 0.14$] and $(Me_3Si)_2O$.

3. Results and discussion

3.1. Synthesis and structures of gold(III) complexes

The reactions of the ligands **1**–**3**, shown in Chart 2, with $Na[AuCl_4]$ were studied. In their deprotonated forms, ligand **1** is expected to act as a bidentate anionic ligand (compare **A**, **B** in Chart 1), while ligands **2** and **3** could act as tetradentate dianionic ligands (compare **C**, Chart 1) or as bidentate anionic ligands (compare **D**, Chart 1).

The ligand **1** did not substitute the chloride ligands of $[AuCl_4]^-$ in neutral or acidic solution, but could react to give the pyridinium salt [PhNHC(=O)–2-C_5H_4NH][$AuCl_4$], **4** (Scheme 1). However, a ligand substitution reaction did occur in the presence of base to give the complex [$AuCl_2(\kappa^2$-*N*,*N*′-PhNC(=O)–2-C_5H_4N)], **5**, according to Scheme 1. Several attempts to prepare the potential complex cation $[Au(\kappa^2$-*N*,*N*′-PhNC(=O)–2-$C_5H_4N)_2]^+$, using excess of the ligand **1** to replace the remaining chloride ligands in **5**, were unsuccessful. Complex **4** retained the yellow color of the $[AuCl_4]^-$ ion, while **5** was red in color, so the successful substitution reaction to give **5** is readily observed.

The structure of complex **4** is shown in Fig. 1. There is hydrogen bonding NH···O=C between pyridinium NH protons and carbonyl groups of neighboring cations, and also hydrogen bonding between the amide NH proton and a chloride ligand of the $[AuCl_4]^-$ anion. The heavy atoms in the cation are roughly coplanar, with the angle between the amide group atoms [N(1)O(1)C(7)C(8)] and the pyridyl and phenyl groups being 6.9° and 3.1° respectively, allowing good π-conjugation.

The structure of complex **5** is shown in Fig. 2. There are two independent, but similar, molecules in the unit cell. As in complex **4**, the amide group is close to planar [e.g. sums of the angles at C(1) and N(1) are each 359.9°], and the gold(III) centers have square planar stereochemistry. The 2-pyridyl group is roughly coplanar with the amide group [twist is 5.7° and 11.9° for the Au(1) and Au(2) molecules respectively], but the phenyl group is twisted out of the amide plane [twist is 65.4° and 71.6° for the Au(1) and Au(2) molecules respectively]. This phenyl twist is necessary to avoid steric interactions with the *cis* chloride ligand, but will reduce π-conjugation with the amide group.

The Au(1) and Au(2) molecules of **5** stack independently through weak intermolecular Au···Cl and, for the Au(2) molecules, Au···O secondary interactions (Fig. 3).

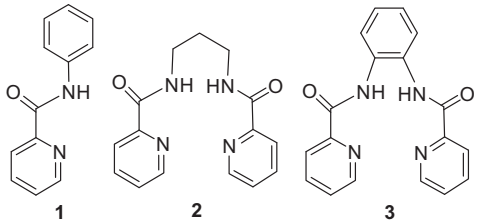

Chart 2. Pyridine-carboxamide ligands.

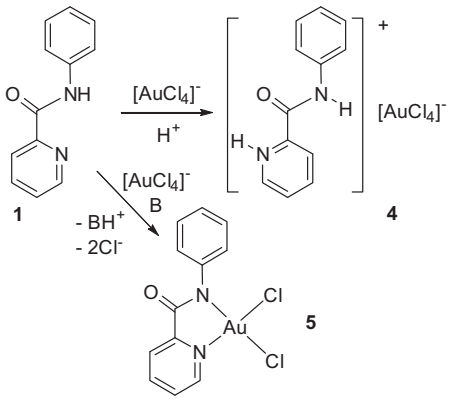

Scheme 1. Synthesis of complexes **4** and **5** (B = base).

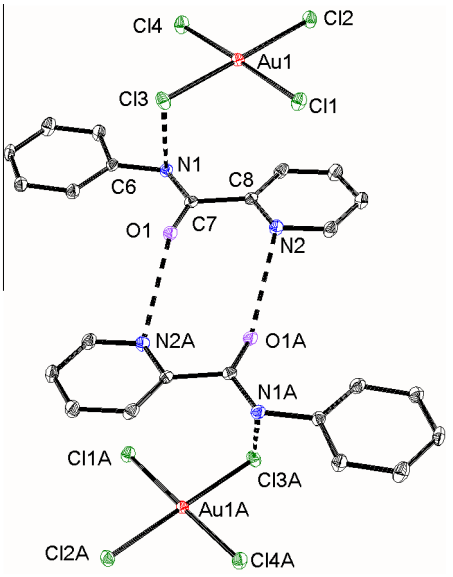

Fig. 1. The structure of complex **4**. Selected bond distances: Au(1)–Cl(1) 2.2810(8), Au(1)–Cl(2) 2.2893(8), Au(1)–Cl(3) 2.2857(8), Au(1)–Cl(4) 2.2778(9), O(1)–C(7) 1.230(4), N(1)–C(7) 1.341(4) Å. H-bond distances: O(1)···N(2A) 2.85, N(1)···Cl(3) 3.53 Å. Symmetry equivalent: A, −*x*, −*y*, −*z*.

The ligands **2** and **3** reacted with $Na[AuCl_4]$ according to Scheme 2. In each case, the product, **6** or **7**, contained the ligand in its bidentate form, with one pyridine-carboxamide arm of the ligand not coordinated to gold(III). Reactions were also carried out using excess $Na[AuCl_4]$, in attempts to form a digold(III) complex with the ligand acting as a bis(bidentate), but these were not successful. In addition, attempts to induce displacement of the remaining chloride ligands in **6** or **7** to give a tetradentate complex analous to **C** (Chart 1), by addition of silver trifluoroacetate, failed to give pure products.

The structure of complex **6** is shown in Fig. 4. The coordination geometry is similar to that in complex **5**, but the supramolecular structure is different. There are hydrogen bonds between NH groups of the free carboxamides and carbonyl groups of coordinated carboxamides to give dimers [R(2,2)(16) in graph theory, N(4)···O(1A) 2.90 Å].

Above and below the gold(III) centers, the shortest intermolecular contacts are Au(1)···Cl(1A) 3.63 Å and Au(1)···Au(1B) 3.88 Å, as shown in Fig. 5. In combination with the hydrogen bonding (Fig. 4), these secondary interactions give rise to a supramolecular network structure.

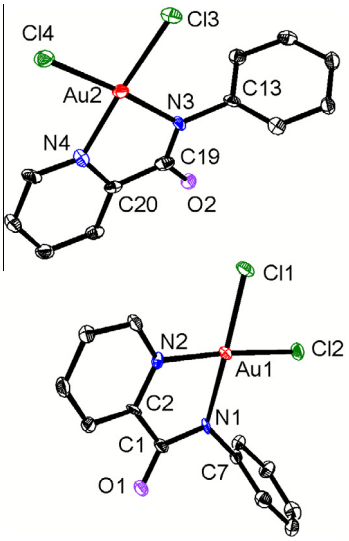

Fig. 2. The structures of the two independent molecules of complex **5**. Selected bond parameters: Au(1)–N(1) 2.018(7), Au(1)–N(2) 2.013(7), Au(1)–Cl(1) 2.288(3), Au(1)–Cl(2) 2.272(2), Au(2)–N(3) 2.006(8), Au(2)–N(4) 2.022(8), Au(2)–Cl(3) 2.265(3), Au(2)–Cl(4) 2.286(3), O(1)–C(1) 1.223(11), O(2)–C(19) 1.242(11), N(1)–C(1) 1.351(11), N(3)–C(19) 1.322(12) Å; N(2)–Au(1)–N(1) 82.2(3)°, Cl(2)–Au(1)–Cl(1) 89.79(10)°, N(3)–Au(2)–N(4) 81.4(3)°, Cl(3)–Au(2)–Cl(4) 89.65(10)°.

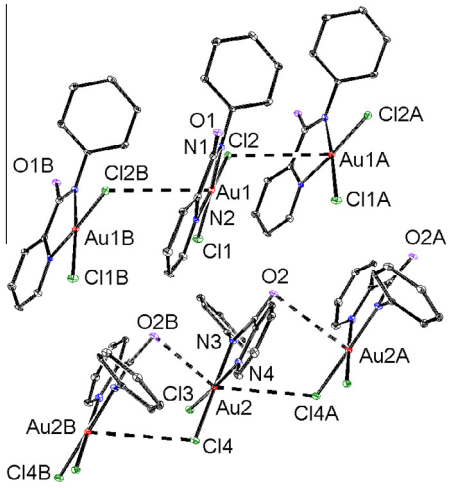

Fig. 3. Secondary bonding interactions in the packing of complex **5**. Selected distances: Au(1)···Cl(2B) 3.80, Au(2)···Cl(4A) 3.75, Au(2)···O(2B) 3.49 Å. Symmetry equivalents: A, $x,½-y,-½+z$; B, $x,½-y,½+z$.

The crystals obtained for complex **7** were always twinned in such a way that detwinning was only partially successful. The structure shown in Fig. 7 is therefore poorly defined. The molecular structure is similar to that for complex **6** (Fig. 4), but there is no intermolecular hydrogen bonding in **7**. As in complex **5** (Fig. 2), the C_6H_4 group is twisted out of the amide plane, by 78° in **7**, to relieve steric hindrance.

3.2. Catalysis

The oxidative α-cyanation of tertiary amines is a useful methodology for C–C coupling steps in organic synthesis [34–43]. A typical procedure is illustrated in Eq. (1) [34], and gives a 98% yield of $PhMeNCH_2CN$ from $PhNMe_2$ when catalyzed by the gold(III) complex $[AuCl_2(bipy)]Cl$ in methanol solvent. With other catalytic systems, different sources of cyanide and different oxidants have been used [35–43] (see Fig. 6).

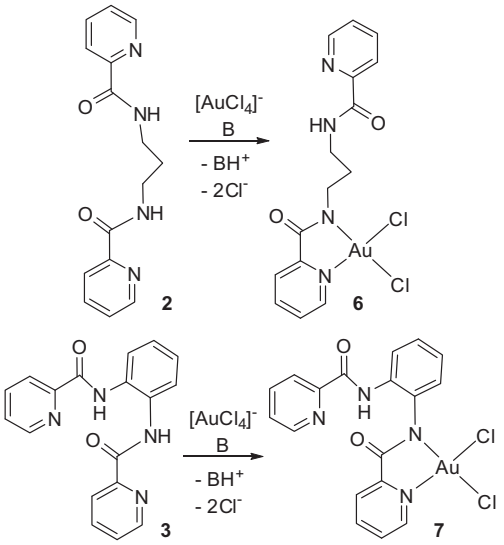

Scheme 2. Synthesis of complexes **6** and **7**.

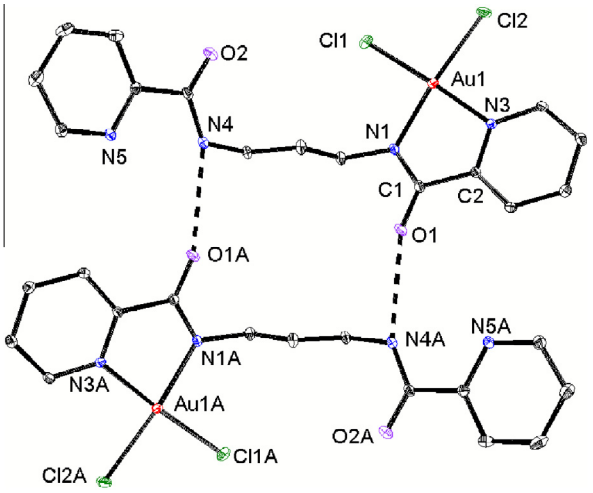

Fig. 4. The structure of complex **6**, showing a pair of hydrogen bonded molecules. Selected bond parameters: Au(1)–N(1) 2.003(2), Au(1)–N(3) 2.036(2), Au(1)–Cl(1) 2.2714(7), Au(1)–Cl(2) 2.2891(7), O(1)–C(1) 1.226(3), N(1)–C(1) 1.347(3), O(2)–C(10) 1.232(3), N(4)–C(10) 1.334(3) Å. Symmetry equivalent: A, $1-x,y,½-z$.

$$PhNMe_2 + Me_3SiCN + {}^tBuOOH \rightarrow PhMeNCH_2CN + Me_2SiOH + {}^tBuOH \quad (1)$$

The mechanism of the catalytic reaction using $[AuCl_2(bipy)]Cl$ was suggested to be as shown in Scheme 3 [34], and involves a gold(III)–gold(V) cycle. The gold cation **E** is oxidized by ^tBuOOH to give an oxogold(V) intermediate **F**. This oxidizes $PhNMe_2$ to the cation radical $[PhNMe_2]^+$, which isomerizes and forms the iminium complex **G**, which then reacts with cyanide to give the product $PhMeNCH_2CN$.

A previous claim of an oxogold complex was made, but was subsequently withdrawn [44], and theory suggests that M = O π-bonding is likely to be weak for late transition metals [45]. Gold(III) tends to form $Au_2(\mu\text{-}O)_2$ linkages rather than terminal Au=O groups [46], while gold(V) oxides have not been characterized. In addition, gold(V) is a difficult oxidation state to access under mild conditions, so this proposed mechanism of Scheme 3 should be reconsidered. DFT calculations, using the BLYP functional with double zeta basis set and scalar relativistic correction [31], were carried out on the proposed intermediate complex **F**. The axial

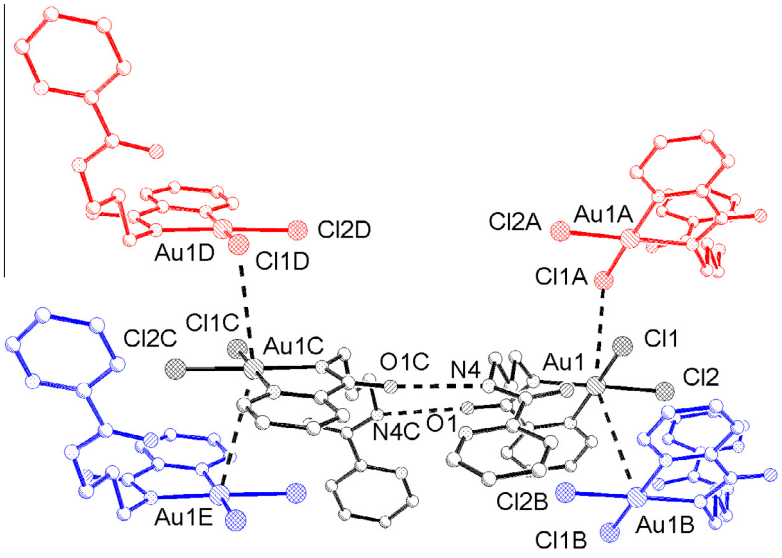

Fig. 5. Part of the network structure of complex **6**, formed by a combination of NH···O=C, Au···Cl and Au···Au secondary interactions. Distances: N(4)···O(1) 2.90, Au(1)···Cl(1A) 3.63, Au(1)···Au(1B) 3.88 Å.

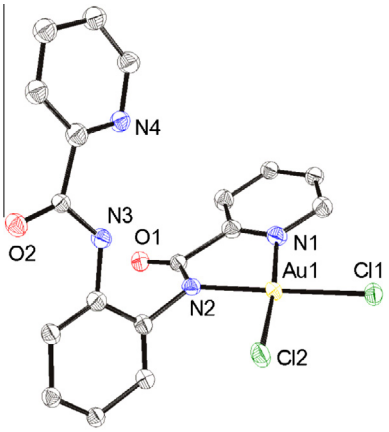

Fig. 6. The structure of complex **7**. Selected bond parameters: Au(1)–N(1) 2.00(3), Au(1)–N(2) 2.00(3), Au(1)–Cl(1) 2.292(8), Au(1)–Cl(2) 2.255(9) Å.

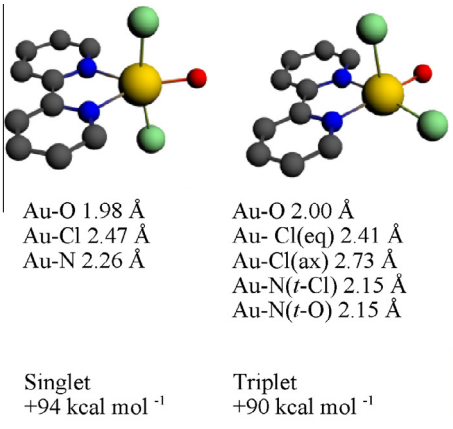

Fig. 7. The calculated lowest energy singlet and triplet state structures for the hypothetical complex $[Au(=O)Cl_2(bipy)]^+$.

oxo stereochemistry **F** is not favored and the more stable structures are a triplet state with equatorial oxo group (better considered as a gold(IV)-oxyl diradical) and a singlet state with

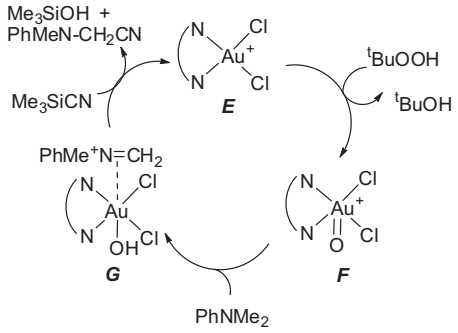

Scheme 3. Proposed mechanism of catalysis of α-cyanation of $PhNMe_2$ from Ref. [34].

trigonal bipyramidal stereochemistry (Fig. 7). The calculated Au–O distances do not indicate multiple bonding (Fig. 7). However, the calculation indicates that the formation of either structure of Fig. 7 by oxidation with ^{t}BuOOH (giving *t*-butanol as co-product) is strongly unfavorable, by at least 90 kcal mol^{-1}, so the mechanism of Scheme 3 is very unlikely under the mild conditions of the catalysis.

The cyanation catalysis was studied, using the conditions reported previously [34], using the neutral complex **5** in place of the reported $[AuCl_2(bipy)]Cl$ catalyst in methanol solution. Similar reactivity was observed, giving $PhMeNCH_2CN$ in 98% yield, based on conversion of $PhNMe_2$, as analysed by GC–MS. The minor product was $PhMeNCH_2CH{=}O$, formed in 2% yield. Under these conditions, no free ligand **1** was detected, indicating that the unit Au(**1**-H) stays intact during the catalysis. The solution became violet-blue in color on addition of $PhNMe_2$ to complex **5**, and the UV–Vis spectrum contained a broad band centered at 590 nm. Oxidation of $PhNMe_2$ with copper(II) in acetonitrile is reported to give the cation radical $PhNMe_2^+$, which is characterized by an absorption band at 470 nm [47,48], while other researchers have suggested that $PhNMe_2^+$ is only formed as a transient intermediate [49]. The species that gives rise to the 590 nm band is probably a radical derived from the transient $PhNMe_2^+$ but its identity is not clear.

The catalysis is not efficient in chloroform solution [34], the maximum yield of $PhMeNCH_2CN$ being 20%, but it was possible

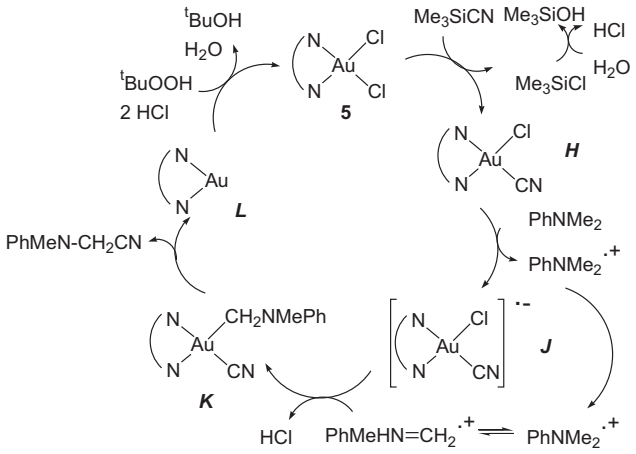

Scheme 4. A possible mechanism for oxidative cyanation.

to obtain insight into the mechanism by monitoring reactions in $CDCl_3$ by ^1H NMR spectroscopy, by UV–Vis spectroscopy and by ESI-MS. Scheme 4 shows a potential reaction mechanism. In individual reactions, complex **5** did not react with the peroxide ^{t}BuOOH but it did react with Me_3SiCN and with $PhNMe_2$. Complex **5** reacted with Me_3SiCN in $CDCl_3$ solution by anion exchange to give Me_3SiCl [identified by its ^1H NMR spectrum, with δ(MeSi) = 0.4 ppm] and the complexes [Au(**1**-H)Cl(CN)], **H**, and [Au(**1**-H)$(CN)_2$], identified by their ESI-MS with m/z = 455 and 446, respectively. Using excess Me_3SiCN, free ligand **1** was also formed, suggesting that cyanide is able to displace **1** from gold(III) under these conditions. Addition of ^{t}BuOOH to this solution led to solvolysis of both Me_3SiCN and Me_3SiCl, with complete displacement of the ligand **1** from gold(III), as monitored by ^1H NMR. Reaction of complex **5** in $CDCl_3$ solution with excess $PhNMe_2$ led immediately to a violet-blue coloration, characterized in the UV–Vis spectrum by a broad band centered at 620 nm. This is tentatively attributed to the same cation radical as observed in methanol, with λ_{max} at 590 nm. The most obvious feature of the ^1H NMR spectrum was that the phenyl resonances of $PhNMe_2$ were shifted and broadened, attributed to easy electron transfer between the cation radical and free $PhNMe_2$. When Me_3SiCN was added to this solution, the blue color was quenched and the phenyl resonances returned to their normal positions. The ^1H NMR spectra also indicated the formation of Me_3SiOH and $(Me_3Si)_2O$ as hydrolysis products. The amine $PhNMe_2$ did not react with *t*-BuOOH so a key role of the gold(III) complex is to oxidize the amine to its cation radical, which appears to be a necessary intermediate.

Both precedent in gold chemistry and the calculations reported above cast doubt on the viability of the proposed gold(III)–gold(V) catalytic cycle of Scheme 3 [34]. Scheme 4 outlines a possible gold(III)–gold(I) catalytic cycle, which is consistent with the experimental data. The gold(III) complex **5** is shown to react with Me_3SiCN to give cyanogold(III) complexes, including complex **H**. It is also shown that complex **5** reacts with $PhNMe_2$, presumably by electron transfer to give the radical cation $[PhNMe_2]^+$ and a gold(II) complex, and so it is reasonable to expect that **H** will react similarly to give a gold(II) complex intermediate **J**. The radical cation/anion pair might then give the gold(III) complex **K**, with loss of HCl. Iminium and imine complexes of gold are often invoked as shortlived intermediates in catalysis, but their nature is not well established [34,50,51]; the σ-bonded form depicted in **K** is speculative since the complex was not directly detected in the reactions, but it is analogous to well known ylide complexes [51–54]. Reductive elimination by C–C bond coupling could give the product and a gold(I) complex [52,55,56], which is then oxidized by ^{t}BuOOH to regenerate **5**. The exact nature of the intermediates is speculative, but the evidence does not support a mechanism involving gold(V). Gold(III)–gold(I) cycles are commonly invoked for other C–C coupling reactions catalyzed by gold complexes [57,58].

Another possible mechanism might involve the intermediacy of digold complexes. In such a mechanism, it could be possible to avoid a paramagnetic gold intermediate **J** and to provide an easier route to reductive elimination of the product, avoiding the strained gold(I) intermediate **L**. Binuclear mechanisms are now well established for palladium(II) and platinum(II) catalysts, for example involving binuclear, diamagnetic $Pd(III)_2$ intermediates, and they can involve amidate bridges [59–63]. The gold(III) catalyst **5** does form π-stacked complexes (Fig. 3), but we have seen no evidence for ligand bridged dimers analogous to the platinum blues and related compounds [63]. Nevertheless, it should be emphasized that Scheme 4 is not the only possible mechanism of catalysis and that a binuclear mechanism is not eliminated.

4. Conclusions

The pyridine-carboxamide ligands, in deprotonated form, bind to gold(III) as bidentate ligands, but the bis(pyridine-carboxamide) ligands do not easily act as tetradentate ligands. In the typical complex [$AuCl_2(\kappa^2$-*N*,*N*′-PhNC(=O)—2-C_5H_4N)], **5**, the gold(III) and the amidopyridine groups are planar, but the phenyl substituent is twisted out of the plane. The neutral complex **5** is an effective catalyst for oxidative cyanation of $PhNMe_2$, with activity comparable to the known cationic catalyst $[AuCl_2(bipy)]^+$ [34]. The detailed mechanism of catalysis is not established, but a cycle involving gold(III), gold(II) and gold(I) complexes is tentatively suggested. The work adds significantly to the known structural and catalytic properties of gold(III) pyridine and amido complexes [1–3,7,8,63–67].

Acknowledgments

We thank the NSERC (Canada) for financial support.

Appendix A. Supplementary data

CCDC 964344–964346 contains the supplementary crystallographic data for complexes **4**–**6**. These data can be obtained free of charge via http://www.ccdc.cam.ac.uk/conts/retrieving.html, or from the Cambridge Crystallographic Data Centre, 12 Union Road, Cambridge CB2 1EZ, UK; fax: +44 1223 336 033; or e-mail: deposit@ccdc.cam.ac.uk.

References

[1] O. Belda, C. Moberg, Coord. Chem. Rev. 249 (2005) 727.
[2] A. Rajput, R. Mukherjee, Coord. Chem. Rev. 257 (2013) 350.
[3] R.W.-Y. Sun, C.-M. Che, Coord. Chem. Rev. 253 (2009) 1682.
[4] M.D. Karkas, T. Akermark, H. Chen, J. Sun, B. Akermark, Angew. Chem., Int. Ed. 52 (2013) 4189.
[5] C.F. Cortney, S.J. Geib, F.-T. Lin, R.E. Shepherd, Inorg. Chim. Acta 358 (2005) 2921.
[6] C.F. Cortney, R.E. Shepherd, Inorg Chem. Commun. 7 (2004) 1065.
[7] A.S.K. Hashmi, Chem. Rev. 107 (2007) 3180.
[8] A. Corma, A. Leyva-Perez, M.J. Sabater, Chem. Rev. 111 (2011) 1657.
[9] S. Nobili, E. Mini, I. Landini, C. Gabbiani, A. Casini, L. Messori, Med. Res. Rev. 30 (2009) 550.
[10] R.J. Puddephatt, Chem. Soc. Rev. 37 (2008) 2012.
[11] T.-C. Cheung, T.-F. Lai, C.-M. Che, Polyhedron 13 (1994) 2073.
[12] D.T. Hill, K. Burns, D.D. Titus, G.R. Girard, W.M. Reiff, L.M. Mascavage, Inorg. Chim. Acta 346 (2003) 1.
[13] S. Wang, Y. Shi, W. Shao, J. Du, H. Wei, J. Zhang, K. Wang, S. Shen, S. Li, J. Li, Y. Zhao, Appl. Organomet. Chem. 26 (2012) 504.
[14] L. Maiore, M.A. Cinellu, S. Nobili, I. Landini, E. Mini, C. Gabbiani, L. Messori, J. Inorg. Biochem. 108 (2012) 123.
[15] T. Yang, C. Tu, J. Zhang, L. Lin, X. Zhang, Q. Liu, J. Ding, Q. Xu, Z. Guo, Dalton Trans. (2003) 3419.
[16] K.J. Kilpin, W. Henderson, B.K. Nicholson, Dalton Trans. (2008) 3899.

[17] S.L. Best, T.K. Chattopadhyay, M.I. Djuran, R.A. Palmer, P.J. Sadler, I. Sovago, K. Varnagy, J. Chem. Soc., Dalton Trans. (1997) 2587.
[18] M. Rossignoli, P.V. Bernhardt, G.A. Lawrance, M. Maeder, J. Chem. Soc., Dalton Trans. (1997) 323.
[19] X.Q. Chen, K.F. Lam, S.F. Mak, K.L. Yeung, J. Hazard. Mater. 186 (2011) 902.
[20] N. Nasser, R.J. Puddephatt, Chem. Commun. 47 (2011) 2808.
[21] N. Nasser, R.J. Puddephatt, Cryst. Growth Des. 12 (2012) 4275.
[22] N. Nasser, A. Borecki, P.D. Boyle, R.J. Puddephatt, Inorg. Chem. 52 (2013) 7051.
[23] T.J. Burchell, D.J. Eisler, R.J. Puddephatt, Chem. Commun. (2003) 2228.
[24] Z. Qin, M.C. Jennings, R.J. Puddephatt, Chem. Eur. J. 8 (2002) 735.
[25] T.J. Burchell, R.J. Puddephatt, Inorg. Chem. 44 (2005) 3718.
[26] N.L.-S. Yue, D.J. Eisler, M.C. Jennings, R.J. Puddephatt, Inorg. Chem. 43 (2004) 7671.
[27] APEX 2, Crystallography software package, Bruker AXS, Madison, WI, 2005.
[28] SAINT, Data Reduction Software, Bruker AXS, Madison, WI, 1999.
[29] G.M. Sheldrick, SADABS v. 2.01, Area Detector Absorption Correction Program, Bruker AXS, Madison, WI, 2006.
[30] G.M. Sheldrick, Acta Crystallogr., Sect. A 64 (2008) 112.
[31] G. te Velde, F.M. Bickelhaupt, E.J. Baerends, S. van Gisbergen, C.F. Guerra, J.G. Snijders, T. Ziegler, J. Comput. Chem. 22 (2001) 931.
[32] R.L. Chapman, R.S. Vagg, Inorg. Chim. Acta 33 (1978) 227.
[33] D.J. Barnes, R.L. Chapman, F.S. Stephens, R.S. Vagg, Inorg. Chim. Acta 51 (1981) 155.
[34] Y. Zhang, H. Peng, M. Zhang, Y. Cheng, C. Zhu, Chem. Commun. 47 (2011) 2354.
[35] M. Rueping, S. Zhu, R.M. Koenigs, Chem. Commun. 47 (2011) 12709.
[36] H.A. Wegner, M. Auzias, Angew. Chem., Int. Ed. 50 (2011) 8236.
[37] L. Liu, Z. Wang, X. Fu, C.-H. Yan, Org. Lett. 14 (2012) 5692.
[38] K.H.V. Reddy, G. Satish, V.P. Reddy, B.S.P.A. Kumar, Y.V.D. Nageswar, RSC Adv. 2 (2012) 11084.
[39] K. Alagiri, K.R. Prabhu, Org. Biomol. Chem. 10 (2012) 835.
[40] G. Yan, J. Yu, L. Zhang, Chin. J. Org. Chem. 32 (2012) 294.
[41] Y. Zhang, S. Luo, C. Zhu, Chin. J. Org. Chem. 32 (2012) 2073.
[42] Y. Li, L. Ma, Z. Li, Chin. J. Org. Chem. 33 (2013) 704.
[43] N. Sakai, A. Mutsuro, R. Ikeda, T. Konokahara, Synlett 24 (2013) 1283.
[44] K.P. O'Halloran, C. Zhao, N.S. Ando, A.J. Schultz, T.F. Koetzle, P.M.B. Piccoli, B. Hedman, K.O. Hodgson, E. Bobyr, M.L. Kirk, S. Knottenbelt, E.C. Depperman, B. Stein, T.M. Anderson, R. Cao, Y.V. Geletii, K.I. Hardcastle, D.G. Musaev, W.A. Neiwert, X. Fang, K. Morokuma, S. Wu, P. Kogerler, C.L. Hill, Inorg. Chem. 51 (2012) 7025.
[45] J.R. Winkler, H.B. Gray, Struct. Bonding (Berlin) 142 (2011) 17.
[46] J.A.T. O'Neill, G.M. Rosair, A.-L. Lee Catal, Sci. Technol. 2 (2012) 1818.
[47] S. Sumalekshmy, K.R. Gopidas, Chem. Phys. Lett. 413 (2005) 294.
[48] M. Kirchgessner, K. Sreenath, K.R. Gopidas, J. Org. Chem. 71 (2006) 9849.
[49] X. Chen, X. Wang, Y. Sui, Y. Li, J. Ma, J. Zuo, X. Wang, Angew. Chem., Int. Ed. 51 (2012) 11878.
[50] A.S.K. Hashmi, L. Molinari, F. Rominger, T. Oeser, Eur. J. Org. Chem. (2011) 2256.
[51] R. Manzano, F. Rominger, A.S.K. Hashmi, Organometallics 32 (2013) 2199.
[52] A. Grohmann, H. Schmidbaur, Comprehensive Organometallic Chemistry II, Vol. 3, Pergamon, 1995.
[53] A.A. Mohamed, H.E. Abdou, J.P. Fackler Jr., Coord. Chem. Rev. 254 (2010) 1253.
[54] J. Vicente, M.T. Chicote, M.C. Lagunas, Helv. Chim. Acta 82 (1999) 1202.
[55] S. Komiya, S. Ozaki, A. Shibue, J. Chem. Soc., Chem. Commun. (1986) 1555.
[56] G.M. Bancroft, T.C.S. Chan, R.J. Puddephatt, Inorg. Chem. 22 (1983) 2133.
[57] M.N. Hopkinson, A.D. Gee, V. Gouverneur, Chem. Eur. J. 17 (2011) 8248.
[58] O.N. Faza, C.S. Lopez, J. Org. Chem. 78 (2013) 4929.
[59] D.C. Powers, T. Ritter, Acc. Chem. Res. 45 (2012) 840.
[60] A.J. Canty, A. Ariafard, M.S. Sanford, B.F. Yates, Organometallics 32 (2013) 544.
[61] K.J. Bonnington, M.C. Jennings, R.J. Puddephatt, Organometallics 27 (2008) 6521.
[62] W.J. Hunks, M.C. Jennings, R.J. Puddephatt, Inorg. Chem. 41 (2002) 4590.
[63] K. Matsumoto, K. Sakai, Adv. Inorg. Chem. 40 (2000) 375.
[64] D. Niedzielska, T. Pawlak, M. Bozejewicz, A. Wojtczak, L. Pazderski, E. Szlyk, J. Mol. Struct. 1032 (2013) 195.
[65] L. Cao, M.C. Jennings, R.J. Puddephatt, Inorg. Chem. 46 (2007) 1361.
[66] M.A. Cinellu, F. Cocco, G. Minghetti, S. Stoccoro, A. Zucca, M. Manassero, J. Organomet. Chem. 694 (2009) 2949.
[67] S. Orbisaglia, B. Jacques, P. Braunstein, D. Hueber, P. Pale, A. Blanc, P. de Fremont, Organometallics 32 (2013) 4153.